Effect of sintering temperature on the structure and electrical properties of KNNS-0.03BNZ ceramics

H. W. Zhao[a,*], Y. L. Li[b], R. J. Zhao[b], Z. Q. Li[c]
[a]*College of Science, North China University of Science and Technology, Tangshan 063210, China*
[b]*Comprehensive test and Analysis Center, North China University of Science and Technology, Tangshan 063210, China*
[c]*Chemical College, Shijiazhuang University, Shijiazhuang 050035, China*

$(K_{0.48}Na_{0.52})NbO_3$-0.03$Bi_{0.5}Na_{0.5}ZrO_3$ (KNNS-0.03BNZ) ceramics were prepared doped with 3 mol% $Bi_{0.5}Na_{0.5}ZrO_3$ (BNZ), and the effect of sintering temperature on dielectric and piezoelectric properties of KNNS-0.03BNZ was also investigated. KNNS-0.03BNZ ceramics at all sintering temperatures exhibit a single perovskite structure, and the change of sintering temperature has no significant effect on the phase composition of KNNS 0.03BNZ ceramics. The Raman shifts of the ν_1 and ν_5 vibration modes have irregular changes in all sintering temperature ranges, indicating that there are polycrystalline phases coexisting in this region. With the change of sintering temperature, T_c slightly shifts to the high temperature direction, and T_{R-T} slightly shifts to the high temperature direction, dielectric constant ε_r continuously increases, while dielectric loss tanδ firstly decreasing and then increasing. Thanks to the presence of a small amount of liquid phase in the ceramics sintered at 1160 ℃, piezoelectric coefficient d_{33} reaches 280 pC/N.

(Received March 21, 2023; Accepted July 10, 2023)

Keywords: Ceramics, Sinter, Dielectric, Piezoelectric

1. Introduction

Piezoelectric ceramics have been widely used in many devices that require electromechanical energy conversion due to their piezoelectric effect [1-3]. Using the positive piezoelectric effect, transducers can be prepared for use in anti-noise telephones, broadband ultrasonic signal transmission systems, etc [4,5]. Piezoelectric actuators can be fabricated using the inverse piezoelectric effect, which plays an important role in the fields of medical ultrasound, shock absorption, and noise reduction, etc [6,7]. Potassium sodium niobate based lead-free piezoelectric ceramics (KNN) are considered to be one of the most likely materials to replace lead zirconate titanate due to their absence of any toxic elements, as well as their high Curie temperature and other superior properties, KNN based ceramics have attracted widespread attention from researchers [8-10]. The piezoelectric constant of pure KNN is 80 pC/N, which is a significant gap compared to lead zirconate titanate (PZT). To completely replace lead based piezoelectric ceramics, their piezoelectric properties need to be further improved.

In the past few decades, researchers have conducted a large amount of research on KNN and made certain progress. Currently, the research on KNN piezoelectric ceramics mainly includes the following aspects: ion doping and phase boundary construction, research on electrical domains, and research on performance stability [11-14]. Through ion doping control, the following four types of polycrystalline phase boundaries have been constructed at room temperature: tripartite-orthogonal phase boundaries (R-O), orthogonal-tetragonal phase boundaries (O-T), tripartite-tetragonal phase boundaries (R-T), and tripartite-orthogonal-tetragonal phase boundaries (R-O-T). The rotation of the electrical domain and the movement of the domain walls are beneficial to improving the piezoelectric response. In addition, the larger the grain size, the less the grain

* Corresponding author: 77110295@qq.com
https://doi.org/10.15251/DJNB.2023.183.813

boundary, and the smaller the resistance to the movement of the electrical domain, which is beneficial to the rotation of the electrical domain, thereby improving the piezoelectric performance [15]. The most traditional method for preparing KNN ceramics is solid-state sintering, which is also the most commonly used preparation method. However, during high-temperature sintering, alkali metal ions can be volatilized, so the volatilization of K^+ and Na^+ during high-temperature sintering is difficult to maintain the stoichiometric composition of KNN materials. In this paper, using $(K_{0.48}Na_{0.52})NbO_3$-$0.03Bi_{0.5}Na_{0.5}ZrO_3$ (KNNS-0.03BNZ) ceramics doped with 3 mol% $Bi_{0.5}Na_{0.5}ZrO_3$ (BNZ) as the substrate, and the sinter was carried out at different temperatures of 1100 ℃, 1120 ℃, 1140 ℃, 1160 ℃, and 1180 ℃, respectively. The effect of sintering temperature on the crystal structure, microstructure, and electrical properties of KNNS-0.03BNZ ceramics was also investigated.

2. Experimental

Accurately weigh the raw materials for each group of experiments according to the stoichiometric ratio, and add the weighed raw materials to a ball milling tank. Add anhydrous ethanol as the ball milling medium for 24 h according to the mass ratio of raw materials: corundum balls: anhydrous ethanol=1:1:2. After the ball milled slurry is dried, put it into a crucible, and calcined at 850 ℃ for 4-6 h. The pre fired powder was ball milled again for 24 h. The slurry after secondary ball milling is dried, ground, and passed through a 200 mesh sieve, then 5% PVA solution is added for granulation, and then passed through a 60 mesh sieve, next, press into a thin sheet with a diameter of 13 mm and a thickness of about 1.3 mm under a pressure of 10 MPa, then, the pressed body was sintered at different temperatures for 3 h, and the sintered ceramic sheet was coated with silver on both sides, and sintered at 600 ℃ for 10 min, finally placed in air for 24 h before its electrical properties were tested.

Conduct phase analysis on the sample using an X-ray diffractometer (XRD, D/max 2500, Rigaku, Japan), and the angle 2θ range from 10 ° to 70 °, and the scanning speed is 10 °/min. Using a scanning electron microscope (SEM, Scios, Chech) to observe the grain size and morphology of the ceramic sample. The Raman spectra of each component of the ceramic were measured using a Raman spectrometer (DXR, Thermo Scientific Nicolet, USA) in the range of wave numbers from 100 to 1000 cm^{-1}, and the evolution process of the ceramic phase structure is judged by analyzing the shift of the characteristic peak Raman shift in the Raman spectrum. Using the LCR 4225 digital bridge meter to obtain the dielectric constant and dielectric loss of the sample at 1 KHz, combined with a temperature control system, the dielectric- temperature curve of the sample was also tested. The piezoelectric coefficient d_{33} of ceramic samples was measured using a ZJ-4A type quasi static tester from the Institute of Acoustics, Chinese Academy of Sciences.

3. Results and discussion

Fig. 1 (a) shows the XRD diffraction patterns of KNNS-0.03BNZ ceramics at different sintering temperatures. KNNS-0.03BNZ ceramics at all sintering temperatures exhibit a single perovskite structure without the formation of other impurity phases, indicating that $(Bi_{0.5}Na_{0.5})ZrO_3$ enters the lattice of KNN based ceramics to form a single solid solution. In order to clearly observe and confirm the phase structure evolution of KNNS-0.03BNZ ceramics with the change of sintering temperature, Fig. 1 (b) shows 2θ enlarged view of the diffraction peak at range from 44° to 47°. From the figure, it can be seen that with the increase of sintering temperature, although the double peaks near 45 ° have a tendency to change towards single peaks, but till the sintering temperature 1180℃, the characteristics of the double peaks can still be seen in the atlas. Therefore, within the range of 1100 ℃ ≤ T ≤ 1180 ℃, KNNS-0.03BNZ ceramics are R-T two-phase

coexistence, and the change of sintering temperature has no significant effect on the phase composition of KNNS 0.03BNZ piezoelectric ceramics.

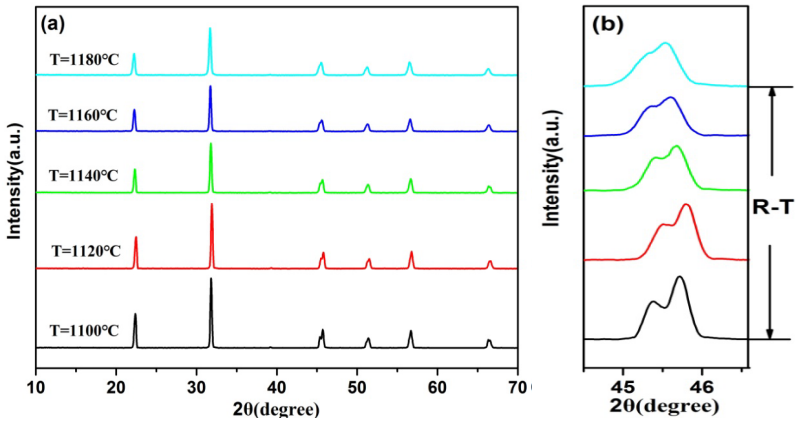

Fig. 1. (a) XRD patterns of the KNNS-0.03BNZceramics at different sintering temperatures and (b) enlarged patterns in the range of 2θ from 44° to 47°.

In order to further confirm the results of X-ray diffraction analysis, Raman spectroscopy tests with a wavenumber range of 100 cm^{-1} to 1000 cm^{-1} were conducted on all samples at different sintering temperatures, as shown in Fig. 2 (a). All vibration modes of NbO_6 are observed from the figure, including $1A_{1g}(\nu_1)+1E_g(\nu_2)+2F_{1u}(\nu_3,\nu_4)+F_{2g}(\nu_5)+F_{2u}(\nu_6)$, proving that the doped ions completely enter the lattice of KNN at various sintering temperatures. Fig. 2 (b) shows the changes in Raman shifts of the ν_1 and ν_5 vibrational modes of KNNS-0.03BNZ ceramics at different sintering temperatures. The changes in the positions of ν_1 and ν_5 peaks are very sensitive to the changes in the phase structure of KNN ceramics, and the occurrence of phase transformation processes can shift the positions of these two peaks. From fig. 2(a), it can be clearly seen that the Raman shifts of the ν_1 and ν_5 vibration modes have irregular changes in all sintering temperature ranges, indicating that there are polycrystalline phases coexisting in this region, which is consistent with the above XRD results.

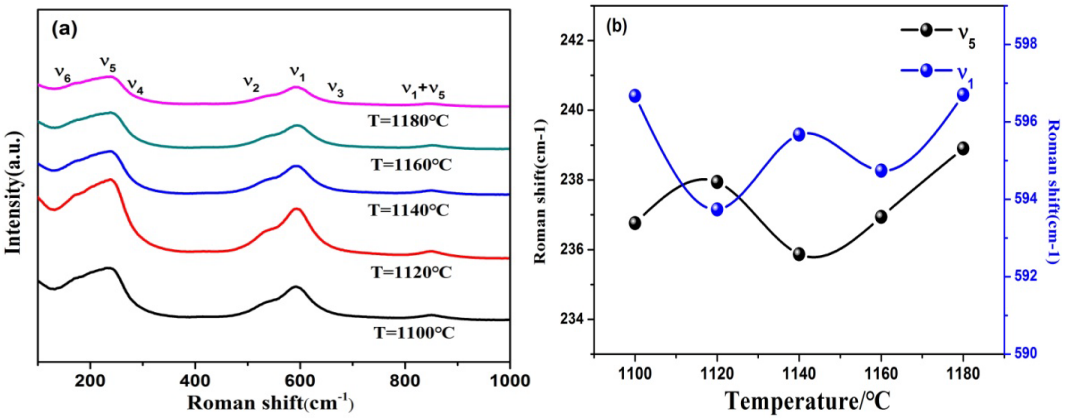

Fig. 2. (a) Raman spectra of KNNS-0.03BNZ ceramics with different sintering temperatures and (b) the changes of ν_1 and ν_5 modes of Raman shift.

Fig. 3 (a) - (e) shows SEM images of KNNS-0.03BNZ ceramics sintered at different temperatures. With the increase of sintering temperature, the ceramic grain size tends to increase first and then decrease, which is because the increase of sintering temperature at low temperatures

provides a higher sintering driving force and promotes the growth of ceramic grains. However, excessive sintering temperature produces a liquid phase that leads to grain refinement. With the continuous increase of sintering temperature, the morphology of ceramic grains is regular and the grain boundaries are obvious when the sintering temperature is below 1160 ℃. When the sintering temperature is equal to 1160 ℃, a small amount of liquid phase is generated in the ceramic sample, the grain rearrangement and strengthened contact improve the grain boundary mobility, and promote the discharge of pores between grains, improving the density of the ceramic [16]. Continue to raise the sintering temperature to 1180 ℃, the ceramics will experience over firing, as can be seen in Fig. 3 (e), a large amount of liquid phase will be generated, and the grain boundaries will also become blurred, then the morphology of the ceramics will deteriorate, which will affect the electrical properties of the ceramics. The results indicate that within a certain sintering temperature range, higher sintering temperatures effectively promote the densification of ceramics in the sintering process.

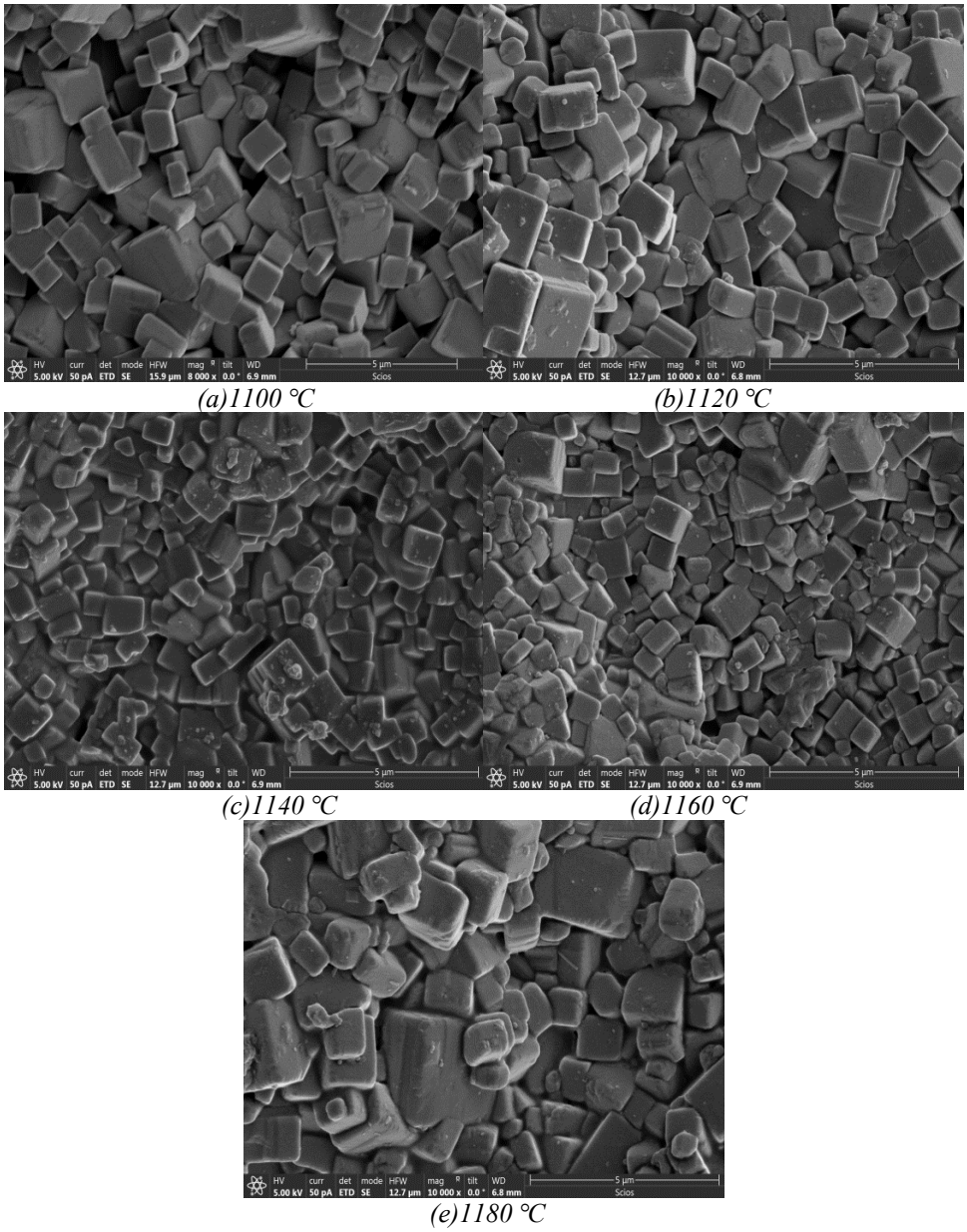

(a)1100 ℃ *(b)1120 ℃*

(c)1140 ℃ *(d)1160 ℃*

(e)1180 ℃

Fig. 3 SEM images and of the KNNS-0.03BNZ ceramics with different sintering temperature and the change of average grain size and density.

Fig. 4(a) shows the dielectric temperature curve of the KNNS-0.03BNZ ceramics measured at 1 kHz in the temperature range from - 50 ℃ to 430 ℃, and Fig. 4(b) shows the dielectric temperature curve of KNNS-0.03BNZ ceramics measured at 1 kHz in the temperature range from - 50 ℃ to 200 ℃. As can be seen from the two figures, all curves have two distinct dielectric peaks corresponding to $T_{R\text{-}T}$ and T_c of the KNN ceramics, respectively. With the change of sintering temperature, T_c slightly shifts to the high temperature direction, and $T_{R\text{-}T}$ slightly shifts to the high temperature direction, which indicates that there is no obvious relationship between the phase transition temperature and sintering temperature. This is consistent with the previous XRD analysis results.

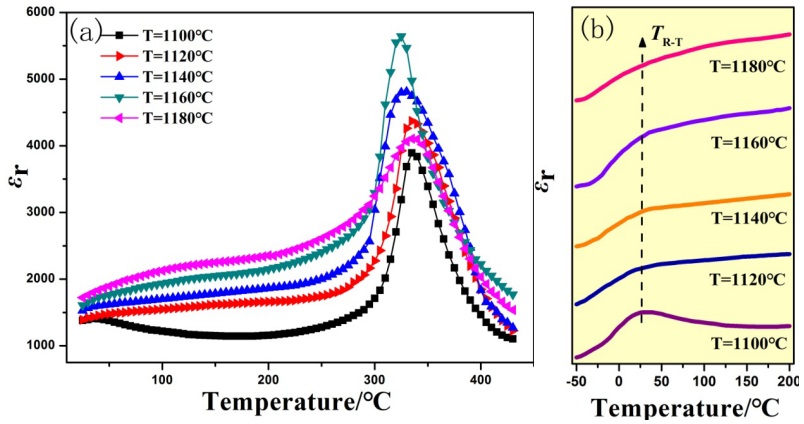

Fig. 4. ε_r-T curves of KNNS-0.03BNZ ceramics with different sintering temperature.

Fig. 5 shows the function of dielectric constant ε_r and dielectric loss tanδ with the sintering temperature measured at 1 kHz and room temperature. As the sintering temperature increases, dielectric constant ε_r continuously increases, while dielectric loss tan δ firstly decreasing and then increasing. This is because as the sintering temperature increases, the density of the sample also increases, thereby increasing the dielectric constant and reducing dielectric loss. However, at excessively high sintering temperatures (1180 ℃), a large amount of liquid phase is generated, resulting in grain refinement, so a decrease in density increases dielectric loss. In addition, too high sintering temperature will accelerate the volatilization of alkali metal ions, making the stoichiometric ratio of the sample unbalanced, which is also detrimental to the improvement of its dielectric properties.

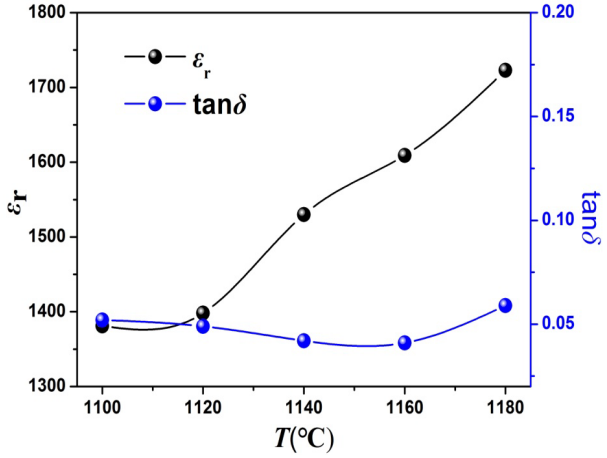

Fig. 5. Function of the ε_r and tanδ with the sintering temperature measured at 1 kHz and room temperature.

Fig. 6 shows the variation of piezoelectric coefficient d_{33} values of KNNS-0.03BNZ ceramics with the sintering temperature measured at 1 kHz and room temperature. With the increase of sintering temperature, the piezoelectric constant d_{33} of ceramic samples continuously increases firstly and then decreases. On the one hand, at a lower sintering temperature (1100 ℃ ~1140 ℃), it provides a higher sintering driving force to promote grain growth and increase the size. A larger grain size is beneficial to the deflection of the electrical domain, thereby improving the piezoelectric properties. On the other hand, the presence of a small amount of liquid phase in the ceramics sintered at 1160 ℃ promotes the grain densification of the ceramics, which also contributes to the improvement of the piezoelectric properties. At excessively high sintering temperatures, the ceramic undergoes overburning and melting, and the microstructure of the ceramic material is damaged. Moreover, the high sintering temperature accelerates the volatilization of alkali metal ions, and in the ABO3 type perovskite structure, a large number of vacancies appear at the A site, resulting in a pinning effect, and thus the piezoelectric properties deteriorate.

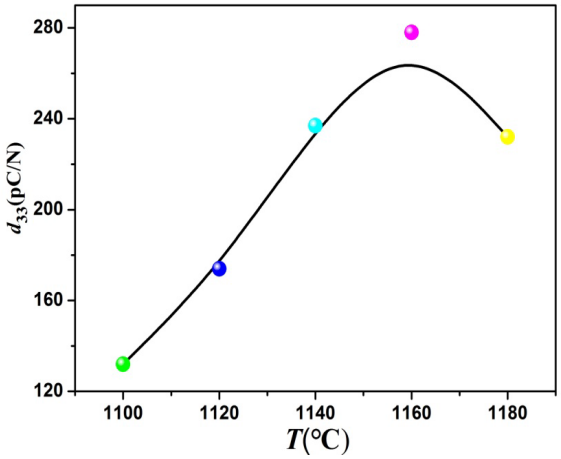

Fig. 6. Variation of d_{33} values of KNNS-0.03BNZ ceramics.

4. Conclusion

Using Na_2CO_3, K_2CO_3, Nb_2O_5, ZrO_2 and Bi_2O_3, et al as starting raw materials, KNNS-0.03BNZ ceramics were prepared, and the effect of sintering temperature on dielectric and piezoelectric properties of KNNS-0.03BNZ was also investigated. The XRD results show that KNNS-0.03BNZ ceramics at all sintering temperatures exhibit a single perovskite structure, and the sintering temperature has no significant effect on the phase composition of KNNS 0.03BNZ ceramics. The Raman analysis and dielectric-temperature results indicate that there are polycrystalline phases coexisting in this region. The sintering temperature has a significant impact on dielectric and electrical properties of ceramics, with the change of sintering temperature, dielectric constant ε_r continuously increases, while dielectric loss tanδ firstly decreasing and then increasing, owing to the presence of a small amount of liquid phase in the ceramics sintered at 1160 ℃, piezoelectric coefficient d_{33} reaches 280 pC/N.

References

[1] F. Jean, F. Schoenstein, M. Zaghrioui, et al, Ceramics International 44, 9463(2018); https://doi.org/10.1016/j.ceramint.2018.02.163

[2] Y.C. Zhen, Z.Y. Cen, L.L. Chen, et al, Journal of Alloys and Compounds 752, 206(2018);

https://doi.org/10.1016/j.jallcom.2018.04.138
[3] G.P. Khanal, I. Fujii, S. Ueno, et al, Journal of the American Ceramics Society 106, 2930(2023); https://doi.org/10.1111/jace.18963
[4] K. Bi, Y.G. Wang, D.A. Pan, et al, Journal of Materials Research 26, 2707(2011); https://doi.org/10.1557/jmr.2011.258
[5] Z.H. Zhou, Y.C. Fan, J.D. Li, Ferroelectrics 197, 647(1997).
[6] R.R. Wang, Y.L. Li, Y. Tian, et al, Digest Journal of Nanomaterials and Biostructures 15, 253(2020).
[7] Y. Sun, S.P. Shen, W.L. Deng, et al, Nano Energy 105, 108024(2023); https://doi.org/10.1016/j.nanoen.2022.108024
[8] B.H. Liu, P. Li, Y. Zhang, et al, Journal of Alloys and Compounds 695, 2207(2016); https://doi.org/10.1016/j.jallcom.2016.11.069
[9] O. Namsar, C. Uthaisar, J. Glaum, et al, Ceramics International 44, 1526(2017); https://doi.org/10.1016/j.ceramint.2017.10.065
[10] X. Lv, J.G. Wu, J.G. Zhu, et al, Journal of the European Ceramic Society 38, 85(2017); https://doi.org/10.1016/j.jeurceramsoc.2017.08.016
[11] T.X. Yan, F.F. Han, S.K. Ren, et al, Materials Research Bulletin 99, 403(2018).
[12] M.H. Zhang, K. Wang, Y.J. Du, et al, Journal of the American Chemical Society 139, 3889(2017); https://doi.org/10.1021/jacs.7b00520
[13] K. Xu, J. Li, X. Lv, et al, Advanced Materials 28, 8519 (2016); https://doi.org/10.1002/adma.201601859
[14] K.B. Xi, Y.L. Li, Z.S. Zheng, et al, Materials Chemistry and Physics 250, 123032(2020).
[15] Y.L. Qin, J.L. Zhang, W.Z. Yao, et al, Acs Applied Materials & Interfaces 8, 7257(2016).
[16] Z. Tan, J.G. Zhu, Y.X. Zhang, et al, Ceramics International 41, 14610(2015); https://doi.org/10.1016/j.ceramint.2015.07.180